L. Marsavina et alii, Frattura ed Integrità Strutturale, 34 (2015) 387-396; DOI: 10.3221/IGF-ESIS.34.43

Focussed on Crack Paths

On the crack path under mixed mode loading on PUR foams

L. Marsavina, E. Linul, T. Voiconi
University Politehnica Timisoara, Romania
liviu.marsavina@upt.ro, tudor_2015@yahoo.com, linul_emanoil@yahoo.com

D. M. Constantinescu, D. A. Apostol
University Politehnica Bucharest, Romania
dan.constantinescu@upb.ro, apostolda@yahoo.com

ABSTRACT. In this paper are presented the crack initiation angles obtained in polyurethane (PUR) foams under mixed mode loading. Closed cell rigid PUR foams having three different densities 100, 145, and 300 kg/m^3 were investigated. Experiments were performed using Asymmetric Semi-Circular Bend and Single Edge Crack specimens.
The obtained crack initiation values were compared with four fracture criteria to introduce: Maximum Tensile Stress, Strain Energy Density, Maximum Energy Release Rate and Equivalent Stress Intensity Factor, and a good agreement was observed. This allow to conclude that the theoretical fracture criteria developed for solid material could be used with success to predict the crack propagation angles in cellular materials like PUR foams.

KEYWORDS. PUR foams; Crack path; Mixed mode.

INTRODUCTION

The main characteristics of polyurethane (PUR) foams are lightweight, high porosity and good energy absorption capacity, [1,2]. One of the main application of foam materials is their utilization as cores in sandwich structures. Of particular interest is the fracture toughness in mixed modes because foam cracking weaknesses the capacity of carrying load of the sandwich structure.
There are several studies to determine the mode I fracture toughness and to investigate the influence of density, loading speed and loading direction [3-11]. A linear correlation between Mode I fracture toughness K_{Ic} and relative density of the foam was observed by Danielsson [7] on PVC Divinycell foams, Viana and Carlsson on Diab H foams [8]. Brittle fracture without yielding in mode I loading was observed by Kabir et al. [9] for PVC and PUR foams applying the procedure described by ASTM D5045. They investigated the effect of density, effect of specimen size, effect of loading rate and effect of cell orientation. Density has a significant effect on fracture toughness, which increases more than 7 times when the foam density increases 3.5 times. Burman [10] presented fracture toughness results for two commercial foams Rohacell WF51 (density 52 kg/m^3) and Divinycell H100 (density 100 kg/m^3). The mode I fracture toughness K_{Ic} was obtained on Single Edge Notch Bending specimens and has values 0.08 MPa·m$^{0.5}$ for WF51, respectively 0.21 MPa·m$^{0.5}$ for H100. He also determined the Mode II fracture toughness using End-Notch Flexure (ENF) specimen with values of 0.13 MPa·m$^{0.5}$ for WF51, respectively 0.21 MPa·m$^{0.5}$ for H100. Poapongsakorn and Carlsson [11] also presented fracture toughness results for PVC foams determined on Three (TPB) and Four Point Bending (FPB), investigating the cell size

and loading rate. Their results show that the value of fracture toughness obtained in FPB loading configuration is higher with a factor of 2 comparing with those obtained on TPB.
Only few studies present the mixed mode fracture of polymeric foams, and only for PVC foams. Hallstträm and Grenestedt [12] investigated mixed mode fracture of cracks and wedge shaped notches in expanded PVC foams. Different types of specimens made of Divinycell H100 were investigated and the non singular T-stress was considered in formulation of fracture criteria. It was concluded that for predominantly mode II the use of T-stress improved the facture predictions. Three different densities of PVC foams were investigated using a Compact Tensile Specimen with Arcan fixtures to produce mixed mode conditions, [13]. The ratio between mode II and mode I fracture toughness K_{IIc}/K_{Ic} was found to be between 0.4 and 0.65 depending on foam density. For mixed mode loading the Richard fracture criterion gives better predictions of fracture limit and crack initiation angle. Marsavina el. al. [14, 15] and Linul et al. [16] presented results mixed mode fracture toughness of PUR foams. They highlighted that the foam density is the major factor influencing fracture toughness, loading speed and loading direction having minor influence. The anisotropy of the foam was explained trough the cellular topology of foams. However, the crack initiation angle is less investigated [13, 15, 16].
Present study assessed the theoretical fracture criteria for crack initiation angle in PUR foam materials under mixed mode loading, using an asymmetric semi-circular bend and single edge crack specimens.

ANALYTICAL MODELS FOR CRACK PROPAGATION

The fracture initiation for a crack in-plane mixed mode conditions is described by:

- The angle of crack initiation θ_c,
- A critical combination of stress intensity factors (K_I and K_{II}) and fracture toughness (K_{Ic}) in the form:

$$F\left(K_I, K_{II}, K_{Ic}\right) = 0 \tag{1}$$

The four most used fracture criterion are summarized below.

Maximum Tensile Stress criterion (MTS)

Erdogan and Sih [17] criterion, based on maximum tensile stress, consider that crack initiation starts radially from the crack tip at an angle $\theta = \theta_c$ perpendicular to the maximum tensile circumferential tensile stress $\sigma_{\theta\theta,max}$. The crack propagation becomes unstable when $\sigma_{\theta\theta,max}$ reaches a critical value σ_{cr}, which is a material parameter at a radius r:

$$\sigma_{\theta\theta,\max} = \sigma_{cr} = \frac{K_{Ic}}{\sqrt{2\pi r}} \tag{2}$$

The equation for crack initiation angle and the relationship between Stress Intensity Factors (SIF's) K_I, K_{II} and fracture toughness K_{Ic} for MTS criterion are presented in Tab. 1.

Condition	Mathematical formulation	
Crack initiation angle	$\theta_c = -\arccos\left(\frac{3K_{II}^2 + K_I\sqrt{K_I^2 + 8K_{II}^2}}{K_I^2 + 9K_{II}^2}\right)$	(3)
$F\left(K_I, K_{II}, K_{Ic}\right)$	$\cos\frac{\theta_c}{2}\left(K_I\cos^2\frac{\theta_c}{2} - \frac{3}{2}K_{II}\sin\theta_c\right) = K_{Ic}$	(4)

Table 1: The MTS criterion.

Minimum Strain Energy Density criterion (SED)

Sih [18] postulated that the fracture occurs in the direction where the strain energy density S is minimum, at a critical distance r_0:

$$S_{cr} = \frac{\kappa - 1}{8\pi\mu}K_{Ic}^2 \tag{5}$$

with μ the shear modulus, $\kappa=3-4\nu$ for plane strain, $\kappa=(3-\nu)/(1+\nu)$ for plane stress, and ν is the Poisson's ratio. Based on SED criterion the crack initiation angle and the relation between K_I, K_{II} and K_{Ic} are presented in Tab. 3.

Condition	Mathematical formulation	
Crack initiation angle	$K_I^2 \sin\theta\left(2\cos\theta+1-\kappa\right)+$ $+2K_I K_{II}\left[\cos\theta(2\cos\theta-\kappa+1)-2\sin^2\theta\right]-K_{II}^2\sin\theta\left(6\cos\theta+1-\kappa\right)=0$	(6)
$F\left(K_I,K_{II},K_{Ic}\right)$	$\frac{1}{2(\kappa-1)}\left[\left(1+\cos\theta_c\right)\left(\kappa-\cos\theta_c\right)K_I^2+2\sin\theta_c\left(2\cos\theta_c-\kappa+1\right)K_I K_{II}+\right.$ $\left.+\left((\kappa+1)\left(1-\cos\theta_c\right)+\left(1+\cos\theta_c\right)\left(3\cos\theta_c-1\right)\right)K_{II}^2\right]=K_{Ic}^2$	(7)

Table 2: The SED criterion.

Condition	Mathematical formulation	
Crack initiation angle	$\frac{\left(\frac{\frac{\theta}{\pi}-1}{\frac{\theta}{\pi}+1}\right)^{\frac{\theta}{\pi}}\cdot\left[6K_I^2\sin\theta\cos\theta-8K_I K_{II}\left(\cos^2\theta-\sin^2\theta\right)-10K_{II}^2\sin\theta\cos\theta\right]}{\left(\cos^2\theta+3\right)^2}+$ $+\frac{4\sin\theta\cos\theta\left(-\frac{\frac{\theta}{\pi}-1}{\frac{\theta}{\pi}+1}\right)^{\frac{\theta}{\pi}}\cdot\left[(3\cos^2\theta+1)K_I^2+8K_I K_{II}\sin\theta\cos\theta+\left(9-5\cos^2\theta\right)K_{II}^2\right]}{\left(\cos^2\theta+3\right)^3}+$ $+\left[\frac{\ln\left(-\frac{\frac{\theta}{\pi}-1}{\frac{\theta}{\pi}+1}\right)\left(-\frac{\frac{\theta}{\pi}-1}{\frac{\theta}{\pi}+1}\right)^{\frac{\theta}{\pi}}}{\pi}-\frac{\theta\left(\frac{1}{\pi\left(\frac{\theta}{\pi}+1\right)}-\frac{\frac{\theta}{\pi}-1}{\pi\left(\frac{\theta}{\pi}+1\right)^2}\right)\left(-\frac{\frac{\theta}{\pi}-1}{\frac{\theta}{\pi}+1}\right)^{\frac{\theta}{\pi}-1}}{\pi}\right]\cdot$ $\cdot\frac{\left[\left(3\cos^2\theta+1\right)K_I^2+8K_I K_{II}\sin\theta\cos\theta+\left(9-5\cos^2\theta\right)K_{II}^2\right]}{\left(\cos^2\theta+3\right)^2}=0$	(9)
$F\left(K_I,K_{II},K_{Ic}\right)$	$4\left(\frac{1}{3+\cos^2\theta_c}\right)^2\left(\frac{1-\frac{\theta_c}{\pi}}{1+\frac{\theta_c}{\pi}}\right)^{\frac{\theta_c}{\pi}}\cdot$ $\cdot\left[\left(1+3\cos^2\theta_c\right)K_I^2+8K_I K_{II}\sin\theta_c\cos\theta_c+\left(9-5\cos^2\theta_c\right)K_{II}^2\right]=K_{Ic}^2$	(10)

Table 3: The Gmax criterion.

Maximum Energy Release Rate criterion (Gmax)

Hussain et al. [19] postulate that the crack propagation initiates when the Energy Release Rate G reaches a critical value G_{Ic} and expressed the energy release rate G in terms of stress intensity factors of initial crack:

$$G(\theta_c) = G_{Ic} = \frac{K_{Ic}^2}{E'} \tag{8}$$

with $E'=E$ Young's modulus for plane stress, and $E'=E/(1-\nu^2)$ for plane strain.
The crack initiation angle could be found by solving Eq. (9) from Tab. 3, while the functional relationship between K_I, K_{II} and K_{Ic} is represented by eq. (10).

Equivalent Stress Intensity Factor criterion (ESIF)

Richard [20, 21] proposed a generalized fracture criterion, based on the equivalent stress intensity factor K_{eq}, which is defined as:

$$K_{eq} = \frac{K_I}{2} + \frac{1}{2}\sqrt{K_I^2 + 4(\alpha K_{II})^2} \tag{11}$$

with $\alpha=K_{Ic}/K_{IIc}$. Crack starts to propagate when K_{eq} reaches the fracture toughness of the material K_{Ic}.
For the crack initiation angle Richard proposed an empirical expression (12), which represents a correlation with a considerable number of experiments.

Condition	Mathematical formulation	
Crack initiation angle	$\theta_c = \mp 155.5^0 \left(\frac{\lvert K_{II}\rvert}{\lvert K_I\rvert + \lvert K_{II}\rvert}\right) - 83.4^0 \left(\frac{\lvert K_{II}\rvert}{\lvert K_I\rvert + \lvert K_{II}\rvert}\right)^2$	(12)
$F(K_I, K_{II}, K_{Ic})$	$\frac{K_I}{2} + \frac{1}{2}\sqrt{K_I^2 + 4(\alpha K_{II})^2} = K_{Ic}$	(13)

Table 4: The ESIF criterion.

MATERIALS AND METHODS

Materials

Crack propagation studies were performed on rigid PUR foams having a closed cell microstructure. Three foam densities, manufactured by NECUMER GmbH (Germany), were investigated 100 kg/m³ (NECURON 100), 145 kg/m³ (NECURON 160) and 300 kg/m³ (NECURON 301). A statistical analysis of the foams microstructure is presented in [14]. The main properties provided by the manufacturer are listed in Tab. 5, [22]. According to the manufacturer the main applications of these foams are test models, draw dies, large volume models, back filling of moulds and patterns, and substructure for hard styling clay.

Property	Units of measure	NECURON		
		100	160	301
Density	kg/m³	100	145	300
Temperature resistance	^{0}C	120	120	65
Compressive strength	MPa	2	3	5
Flexural strength	MPa	1.5	2.5	6

Table 5: Material properties according to manufacturer [22] (approximate values).

Determination of density

The density determination of the considered foams was performed according with ASTM D 1622-03 [23]. A Sartorius GD 503 Class Balance was used for the mass determination, and the dimensions of the specimens (84 x 35 x 10 mm) were measured using a digital caliper Mitutoyo Digimatic.

Fracture toughness determination and mixed mode loading tests

The fracture toughness K_{Ic} and K_{IIc} of PUR foams were determined using two types of specimens: Asymmetric Semicircular Bend (ASCB) and Single Edge Crack (SEC), Fig. 1. The choice of using these specimen types was that with the same shape is possible to produce from pure mode I loading to pure mode II loading, and intermediate mixed modes only by changing the position S_2 of one support for ASCB specimens or by changing the loading direction β for SEC specimens. The ASCB specimen with radius R, which contains an edge crack of length a oriented normal to the specimen edge, loaded with a three point bend fixture, was proved to give a wide range of mixed modes from pure mode I ($S_1=S_2$) to pure mode II ($S_1 \neq S_2$), only by changing the position of one support. The considered geometry of the specimen has: R=40 mm, a=20 mm, t=10 mm, $S_1 = S_2$=30 mm (for symmetric loading and mode I fracture toughness determination), 12 mm, 8 mm, 6 mm, 4 mm (for mixed mode loading) and S_2=2.66 mm (for mode II fracture toughness determination). The dimensions of the SEC specimens were W = 75 mm, t = 8 mm and a = 33.75 mm and the loading angle was $\beta = 0^0$ for mode I tests, 30^0, 45^0, 60^0 for mixed mode loading, respectively $\beta = 90^0$ for mode II tests.

Tests were carried out at room temperature (20 ^{0}C) on a 5 kN Zwick Proline testing machine, using displacement control with 2 mm/min loading speed, Fig. 2. Typical load - displacement curves are shown in Fig. 3: a. the effect of applied mixed mode on ASCB specimens for the foam with density 145 kg/m^3, and b. the influence of density on SEC specimens loaded in mode I. All tested specimens show a linear behaviour and a brittle fracture, which was confirmed by the fact that no plastic deformations remain after testing.

The determination of fracture toughness is presented in more detail in [14, 15] for ASCB specimens and in [16] for SEC specimens. The experimental results for density and fracture toughness of investigated foams are presented in Tab. 6. It should be mentioned that the fracture toughness results are determined for specimens obtained in the rise direction (in plane). A discussion regarding the foams anisotropy is presented elsewhere, [14].

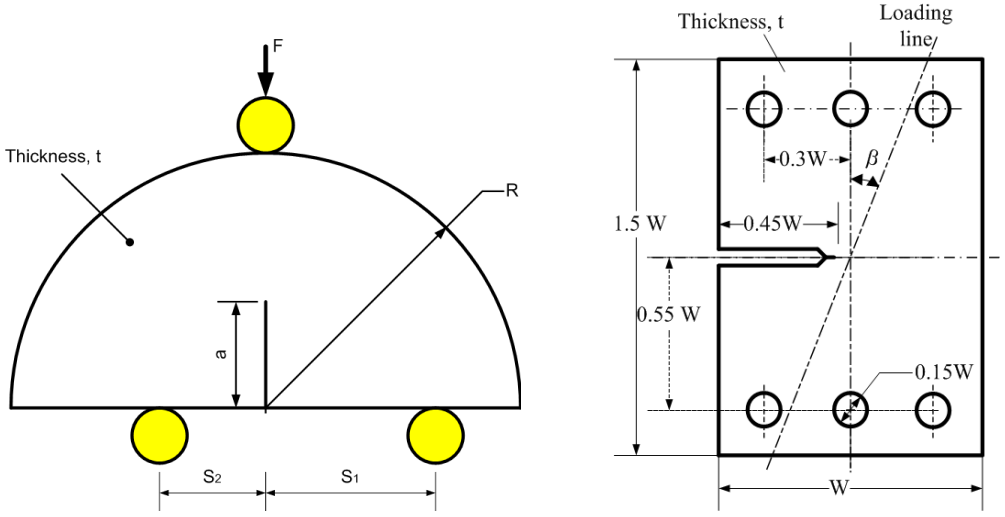

a. ASCB specimen b. SEC specimen

Figure 1: Specimens used from fracture toughness and mixed mode loading tests.

It could be observed that fracture toughness K_{Ic} and K_{IIc} increases with density. The maximum relative differences between fracture toughness values obtained by ASCB and SEC specimens was 28% for foam with density 100 kg/m^3 for mode II, while minimum relative difference was obtained for the same density for K_{Ic} 1.1%. Also, it could be observed that the mode II fracture toughness values are lower than the mode I ones for all foam densities and specimen type, with the exception of 300 kg/m^3 foam density using ASCB specimens.

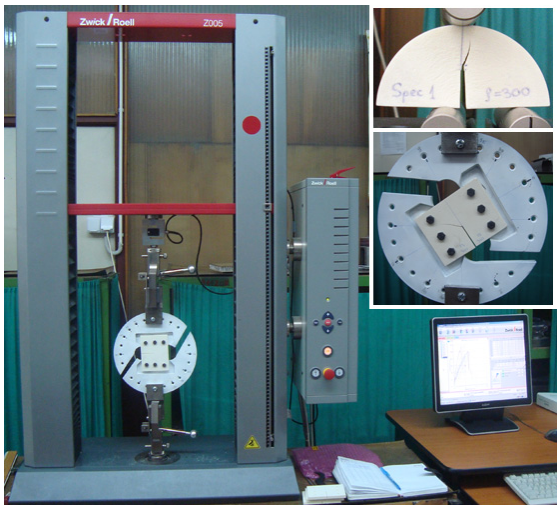

Figure 2: Experimental set - up with details of ASCB specimen in three point bending grips (top right), respectively with SEC specimen in Arcan grips (left and middle right).

Property	Units of measure	NECURON		
		100	160	301
Density	kg/m³	100.35±0.25*	145.53±0.22*	300.28±1.38*
Mode I fracture toughness (ASCB)	MPa·m$^{0.5}$	0.087	0.131	0.372
Mode II fracture toughness (ASCB)	MPa·m$^{0.5}$	0.049	0.079	0.374
Mode I fracture toughness (SEC)	MPa·m$^{0.5}$	0.088	0.108	0.337
Mode II fracture toughness (SEC)	MPa·m$^{0.5}$	0.069	0.095	0.319

Table 6: Material properties determined experimentally (* standard deviation values).

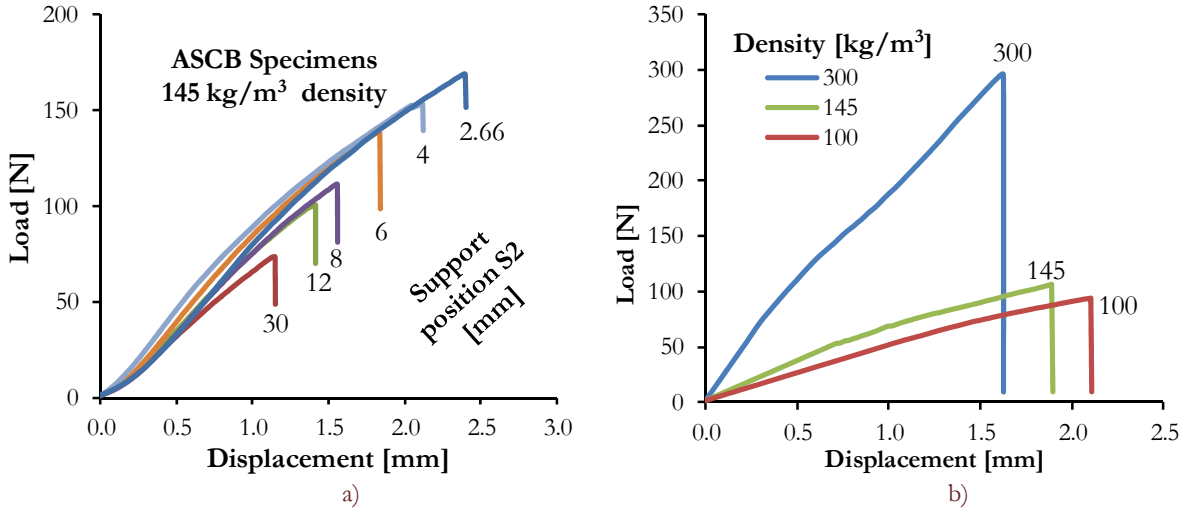

Figure 3: Typical load - displacement curves: a) Influence of applied mixed mode for ASCB specimens; b) Influence of density for SEC specimens loaded in Mode I.

RESULTS AND DISCUSSIONS

This paper is focused on the determination the crack initiation angle and the obtained crack paths under mixed mode loading of PUR foams.

The obtained crack paths were digitized using a NIKON D5100 Digital Camera. Fig. 4 presents the crack paths for ASCB specimens for six loading configurations: a. mode I, b.-e. mixed modes, f. mode II. Except for the mode I case, when the crack propagates like a straight line, all other cases show curvilinear crack paths.

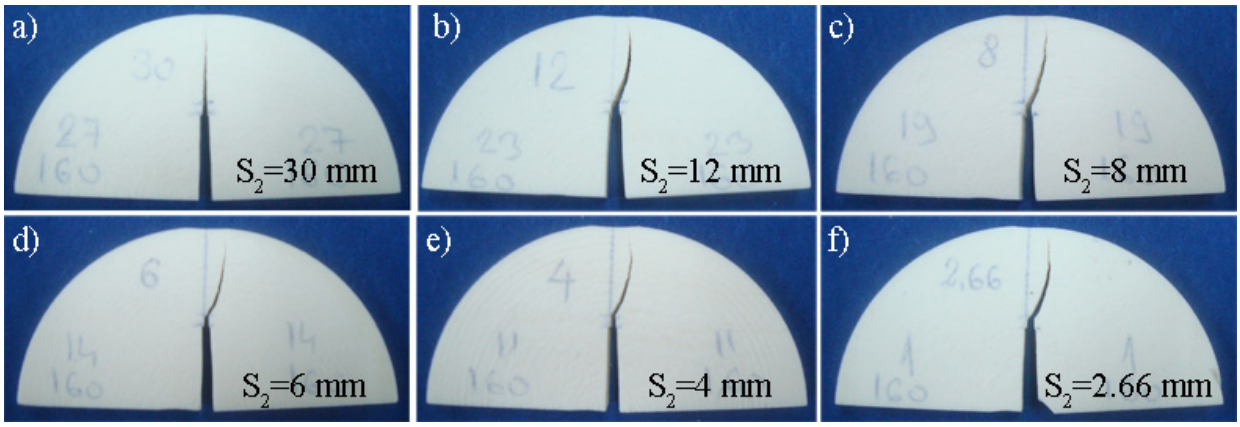

Figure 4: Crack paths resulted from testing ASCB specimens.

In Fig. 5 the crack paths for SEC specimens are shown. More straight crack trajectories resulted on testing the SEC specimens for all loading configurations.

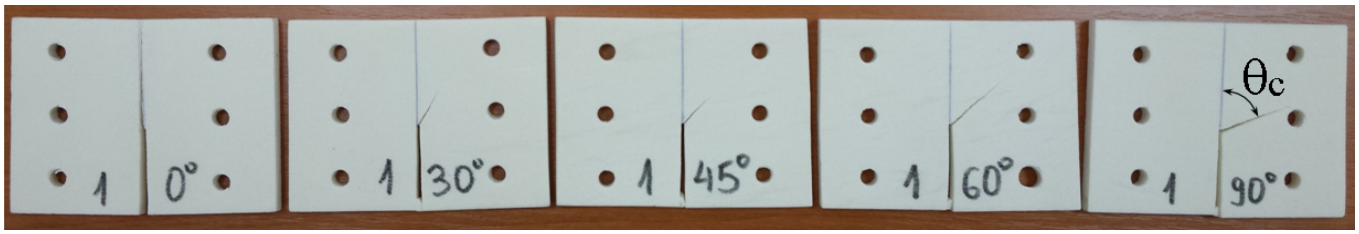

a. β = 0 °C b. β = 30 °C c. β = 45 °C d. β = 60 °C e. β = 90 °C

Figure 5: Crack paths resulted from testing SEC specimens.

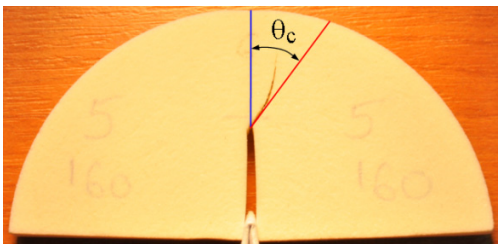

Figure 6: Measurement of crack initiation angle.

The crack initiation angle θ_i was measured on each specimen using Sigma Scan Pro software as the angle between the tangent (red line) to the crack at the initiation point and the crack initial direction (blue line) in Fig. 6.

Fig. 7 presents the mean values and the range (minimum to maximum values) of the crack initiation angle θ_i measured on the specimens versus applied mixed mode loading $Me = Arctg(K_{II}/K_I)$ side by side with the predicted crack propagation angles by the four theoretical criteria. It could be observed that for predominantly mode I loadings $Me < 45^0$ the measured values are in good agreement with the predicted ones. For predominantly mode II loading ($Me > 45^0$) the

experimental crack propagation angles differ from the predicted values. It can be also observed that the foam with density 300 kg/m³, with a microstructure close to a porous solid gives closer propagation angles to theoretical predictions (especially to MTS and ESIF), developed for brittle solid materials. Noury et al. [13] also found, investigating PVC foams in mixed mode loading, that MTS criterion gives the closest crack initiation angles to experimental values. Comparing the two type of specimens the crack initiation angles obtained on SEC specimens are above those results for testing ASCB specimens, and closer to the theoretical predictions.

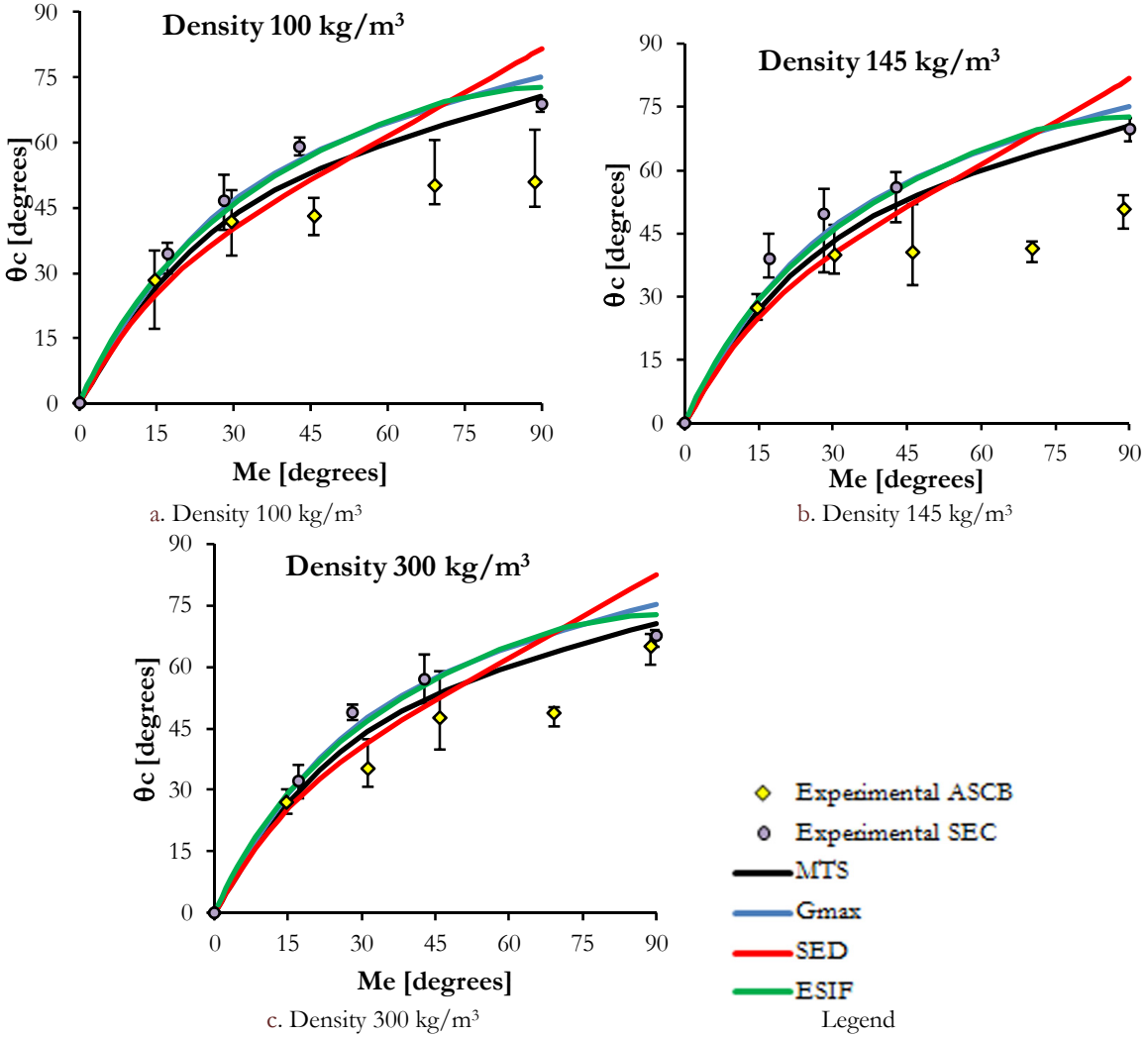

a. Density 100 kg/m³ b. Density 145 kg/m³

c. Density 300 kg/m³ Legend

Figure 7: Comparison between experimental and theoretical crack initiation angles.

In order to investigate the effect of density, the mean value of crack initiation angle is plotted versus the support position S_2 for ASCB specimens in Fig. 8.a, respectively versus loading angle β for SEC specimens, Fig. 8.b. The crack initiation angles are slightly different for the investigated densities. This is more pronounced for ASCB specimen, where maximum relative difference between densities 145 and 300 kg/m³ and mode II loading (S_2=2.66 mm) is 22.3%. The maximum relative difference for SEC specimens was observed for loading angle $\beta = 30^0$ is 7.2% and this could be considered in the range of experimental determination.

CONCLUSIONS

Crack initiation angle on mixed mode loading for PUR foams of three different densities was investigated experimentally. Two specimens ASCB and SEC were considered, which allow to produce mixed mode loading only by changing some loading configurations. The obtained values were compared with four most used fracture

criteria MTS, SED, Gmax, respectively ESIF, and a good agreement was observed. This allows to conclude that the theoretical fracture criteria developed for a solid material could be used with success to predict the crack propagation angles in cellular materials like PUR foams.
Crack paths presented in Figs. 4 and 5 show that crack initiates in mixed mode or mode II, but grows to regain the symmetry and to eliminate mode II.

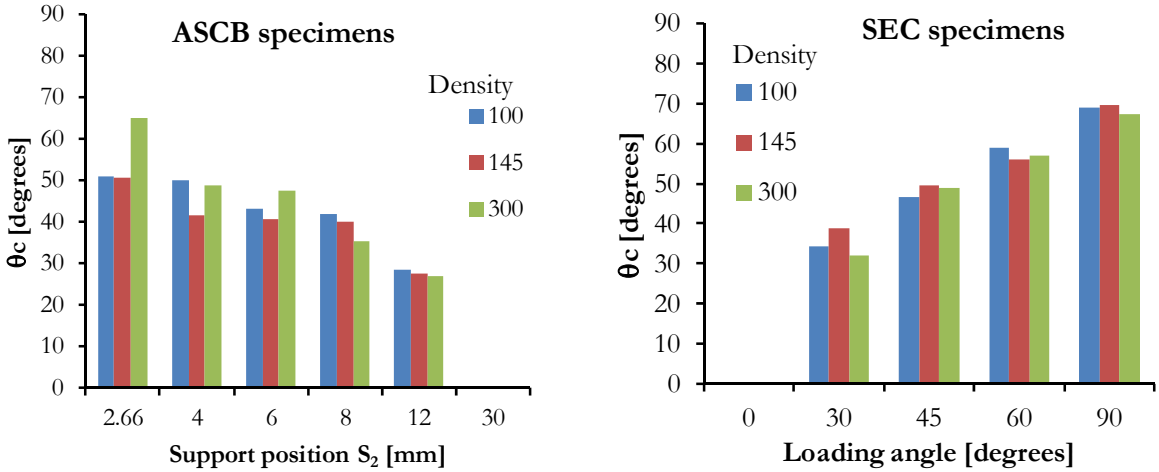

a. ASCB specimens b. SEC specimens

Figure 8: Effect of density on crack initiation angle.

ACKNOWLEDGMENTS

This work was supported by a grant of the Romanian National Authority for Scientific Research, CNCS – UEFISCDI, project PN-II-ID-PCE-2011-3-0456, contract number 172/2011. Dr. E. Linul was partially supported by the strategic grant POSDRU/159/1.5/S/137070 (2014) of the Ministry of National Education, Romania, co-financed by the European Social Fund – Investing in People, within the Sectoral Operational Programme Human Resources Development 2007-2013. Dr. D.A. Apostol was partially supported by the strategic grant POSDRU/ POSDRU/159/1.5/S/137390/ (2014) of the Ministry of National Education, Romania, co-financed by the European Social Fund – Investing in People, within the Sectoral Operational Programme Human Resources Development 2007-2013.

REFERENCES

[1] Gibson, L.J., Ashby, M.F., Cellular solids, structure and properties, Second edition, Cambridge University Press, (1997).
[2] Srivastava, V., Srivastava, R., On the polymeric foams: modeling and properties, J. Mater. Sci., 49 (2014) 2681-2692.
[3] Marsavina, L., Fracture mechanics of foams, in H. Altenbach, A. Ochsner (Eds.), Cellular and porous materials in structures and processes, Springer, Wien, (2010) 1-46.
[4] Marsavina, L., Constantinescu, D.M., Failure and damage in cellular materials, in H. Altenbach, T. Sadowski (Eds.), Failure and damage analysis of advanced materials, Springer, Wien, (2015) 119-190.
[5] Huang, J.S., Gibson, L.J., Fracture toughness of brittle foams, Acta Metall. Mater., 39 (1991) 1627-1636.
[6] Choi, S., Sankar, B.V. Fracture toughness of carbon foam, J. Compos. Mater., 37 (2003) 2101-2116.
[7] Danielsson, M., Toughened rigid foam core material for use in sandwich construction, Cell. Polym., 15 (1996) 417-435.
[8] Viana, G.M., Carlsson, L.A., Mechanical properties and fracture characterisation of cross-linked PVC foams, J. Sandw. Struct. Mater., 4 (2002) 91-113.
[9] Kabir, M.E., Saha, M.C., Jeelani, S., Tensile and fracture behavior of polymer foams, Mat. Sci. Eng. A-Struct., 429 (2006) 225-235.

[10] Burman, M., Fatigue crack initiation and propagation in sandwich structures, Report No.98-29, Stockholm (1998).
[11] Poapongsakorn, P., Carlsson, L.A., Fracture toughness of closed-cell PVC foams: effect of loading configuation and cell size, Compos. Struct., 102 (2013) 1-8.
[12] Hallstrom, S., Grenestedt, J.L., Mixed mode fracture of cracks and wedge shaped notches in expanded PVC foam, Int. J. Fract, 88 (1997) 343-358.
[13] Noury, P.M., Shenoi R.A., Sinclair, I., On mixed-mode fracture of PVC foam, I J Fracture, 92 (1998) 131-151.
[14] Marsavina, L., Constantinescu, D.M., Linul, E., Apostol, D.A., Voiconi, T., Sadowski, T., Refinements on fracture toughness of PUR foams, Eng. Fract. Mech., 129 (2014) 54-66.
[15] Marsavina, L., Constantinescu, D.M., Linul, E., Voiconi, T., Apostol, D.A., Sadowski, T., Evaluation of mixed mode fracture for PUR foams, Procedia Materials Science, 3 (2014) 1342-1352. DOI:10.1016/j.mspro.2014.06.217.
[16] Linul, E., Voiconi, T., Marsavina, L., Determination of mixed mode fracture toughness of PUR foams, Structural Integrity and Life, 14 (2014) 87-92.
[17] Erdogan F., Sih G. C., On the crack extension in plates under plane loading and transverse shear, J Basic Engng, 85 (1963) 519-525.
[18] Sih G. C., Strain-energy-density factor applied to mixed mode crack problems, I J Fract, 10 (1974) 305-321.
[19] Hussain M. A., Pu S. L., Underwood J., Strain energy release rate for a crack under combined mode I and mode II. In: Fracture analysis, P.C. Paris, G.R. Irwin (Edts), ASTM STP560, Philadelphia, (1974) 2-28.
[20] Richard H. A., Bruchvorhersagen bei uberlagreter normal- und schubbeanspruchung von rissen, VDI-Verlag, Dusseldorf, (1985).
[21] Richard H. A., Fulland M., Sander M., Theoretical crack path prediction, Fatigue Fract Engng. Mater. Struct., 28 (2005) 3-12.
[22] http://necumer.com/index.php/en/produkte-2/board-materials/modelling, (2014).
[23] ASTM D1622-03 Test Method for Apparent Density of Rigid Cellular Plastics.